

Combining NMR and molecular modelling in a drug delivery context: investigation of the multi-mode inclusion of a new NPY-5 antagonist bromobenzenesulfonamide into β -cyclodextrin

Gloria Uccello-Barretta,^{a,*} Federica Balzano,^a Giuseppe Sicoli,^a Carmen Frígola,^b Ignacio Aldana,^b Antonio Monge,^b Donatella Paolino^c and Salvatore Guccione^{c,*}

^aDipartimento di Chimica e Chimica Industriale, Università degli Studi di Pisa, via Risorgimento 35, 56126 Pisa, Italy

^bUnidad de I+D de Medicamentos. CIFA. Universidad de Navarra. 31008 Pamplona, Spain

^cDipartimento di Scienze Farmaceutiche, Università degli Studi di Catania, V.le A. Doria 6, Ed. 2 Città Universitaria, I-95125 Catania, Italy

Received 25 July 2003; accepted 17 October 2003

Abstract—NMR spectroscopic and molecular modelling methods have been employed to describe the complexation of *trans*-*N*-4-[*N'*-(4-chlorobenzoyl)hydrazinocarbonyl]cyclohexylmethyl-4-bromobenzenesulfonamide, a new chemotype of NPY-5 antagonist, and β -cyclodextrin, revealing the coexistence of two different kinds of 1:1 complexes where conformational changes of the guest compound with respect to the free state are also detected

© 2003 Elsevier Ltd. All rights reserved.

1. Introduction

Neuropeptide Y (NPY), a highly conserved 36 amino acid polypeptide that is widely distributed throughout the central and peripheral nervous system, is involved in the regulation of a variety of neuroendocrine functions. These effects are mediated through activation of a family of G-protein coupled receptors (known as Y1–Y6). There is evidence that NPY-5 receptor may play an important orexigenic role in feeding response in rodents. Selective Y5 antagonists could become promising anti-obesity agents without the cardiovascular side effects¹ or at least useful tools to elucidate the role of NPY-5 sub-type receptor.^{1–5}

Modern drug design not only focuses on the pharmacological activity of a drug like compound but also considers its ability to be absorbed and to reach its site of action. Since the *peroral* route for drug administration is the most convenient and preferred by patients, the main objective in the process of drug development is to obtain a drug product with a good oral bioavail-

ability. Poor pharmacokinetic properties, such as low oral absorption, have been associated with 40% of drug failures.⁶ Molecular host-guest based systems are prime candidates for regulating a drug's rate release in the body. A very popular hosts family is constituted by cyclodextrins (CDs), used to improve solubility and bioavailability of poorly water-soluble compounds and a matter of interest to pharmaceutical applications since these compounds can spontaneously form inclusion complexes with a variety of guest molecules in aqueous media.⁷ This property originates from their unique 'toroidal' structure, that is, a basked-type shaped central cavity of 0.6–1 nm in diameter, which can be described as a truncated cone, endowed with a polar external surface, responsible for their solubility in aqueous means, and with an internal apolar cavity, where the displacement of water molecules by hydrophobic guests and, hence, their inclusion is a process thermodynamically favoured.⁸ The above features are clearly displayed by the GRID (version 21)^{9–11} and HINT 2.35S (shortcut for **H**ydrophobic **I**nteractions)^{12,13} maps (Figs 1 and 2), the latter as implemented in Sybyl 6.9.¹⁴ The unexpectedly less pronounced hydrophobic contours down the middle of the CD structure suggest that the polar influence of the hydroxyl oxygens extends right towards the middle of the molecule. As a countercheck some of the GRID (version 21)^{9–11} water contours, also tend to

* Corresponding authors. Tel.: +39-050-221-9232; fax: +39-050-221-9260 (G. U.-B.); tel.: +39-095-738-4020; fax: 39-095-443-604 (S. G.); e-mail addresses: gub@dccl.unipi.it; guccione@unict.it.

occur down the middle of the CD structure, for instance at an energy of -5 kcal/mol there is still a lot of water contour.

Cyclodextrin complexes in which aromatic amino acids are involved are of interest as chiral selectors^{15,16} and models for enzyme-substrate specific binding.^{8,17}

There are three basic structures that differ only in the number of units. The α -cyclodextrin (α -CD), of six units, the β -cyclodextrin (β -CD) of seven units and the γ -cyclodextrin (γ -CD) of eight units connected through α -1,4 chemical bonds. Complexation processes in solution depend on the size, shape and hydrophobicity of the guest molecule and are accompanied by an increase in the strain in the CD cavity.⁸ The main forces that have to do with the complexation processes are van der Waals interactions between guest and host, responsible for the stability of complexes in water and in vacuo, and hydrophobic interactions for the case of aqueous solutions. Other important interactions are hydrogen bonding between the guest and the hydroxyl groups of the CD, release of strain energy in the molecule ring and dipole-dipole and/or coulombic interactions.^{8,17}

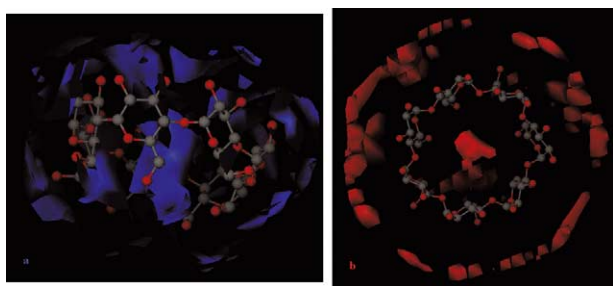


Figure 1. GRID 21^{9–11} maps of the β -cyclodextrin structure as retrieved from the Cambridge Structural Database (CSD)^{32–34} version 5.24, November 2002. Data updates April 2003. CSD code: BCDEXD03 or BISTAY. The co-crystallized ligand was extracted before the analysis (see Experimental). (a) blue contours (-4.6 kcal/mol): polar (water) map (side view); (b) red contours (-0.035 kcal/mol): hydrophobic probe map (front view). A central tunnel down the centre of the big toroidal structure is clearly displayed.

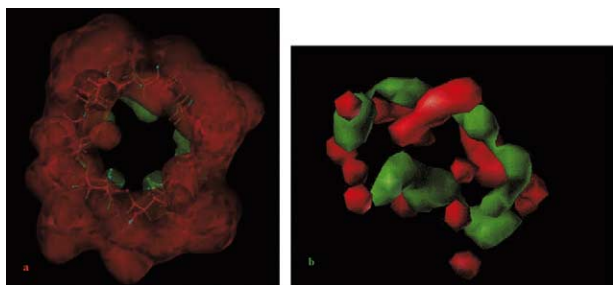


Figure 2. (a) HINT 2.35S^{12–14} hydropathicity map of the β -cyclodextrin structure as retrieved from the Cambridge Structural Database (CSD)^{32–34} (version 5.24, November 2002. Data updates April 2003. CSD code: GETPAW). The co-crystallized ligand was extracted before the analysis (see Experimental). The external hydrophilic (red) and internal (green) apolar areas are displayed. (b) HINT 2.35S^{12–14} hydropathicity map of a *disordered* (not toroidal) β -cyclodextrin structure obtained by manually building from the fragments as in the SYBYL 6.8 and 6.9 BIOPOLYMER module¹⁴ and roughly minimizing to emphasize the *double face* character of the molecule. The binding cavity shows very visual hydrophobic properties. A guest could bind in the center, even if it is hydrophobic (green contours).

In view of the relevance of these applications, a detailed knowledge of the dynamics and host-guest orientation of inclusion complexes formed by cyclodextrins constitutes the basis for their use as drug carriers, *prior* to a possible further development of drugs. In this context we have exploited NMR spectroscopy and molecular modelling methods in order to give a defined picture of the complexation phenomena involving cyclomaltoheptaose (β -cyclodextrin, β -CD) and the sodium salt of *trans*-*N*-{4-[*N'*-(4-chlorobenzoyl)hydrazinocarbonyl]-cyclohexylmethyl}-4-bromobenzenesulfonamide (**G-Na**), being the parent compound **G** (Fig. 3) a representative of potent and selective *N'* substituted carbohydrazides acting as hNPY-5 antagonists (in vitro: NPY hY5 K_i nM 4.30, no affinity for the hNPY Y1 receptor, i.e., K_i values were higher than 10^{-5} M), possible *drugability* of which is negatively affected because of a poor water solubility at a pH of 5–7 (<0.1 mg/mL). Preliminary ‘in vivo’ evaluation (data not shown) showed promising results.

The quantitative analysis of the dependence of proton chemical shifts on the drug/cyclodextrin molar ratio has been used as the basis for defining the complexation stoichiometry,¹⁸ as well as the detection of dipolar interactions by NOE¹⁹ or proton selective relaxation methods²⁰ has been employed for imposing the conformational restraints needed to define the stereochemistry and dynamics of the cyclodextrin complexes formed in solution.

Conformational in vacuo and *aqueous* analysis using the software MacroModel (version. 8.0)^{21,22} as implemented in the MAESTRO suite (version. 5.0)²² and high level quantum chemical calculations (HF-MIDI^{23,24} and Jaguar version 4.0 release 23²²) were carried out to complement the NMR results and have a definite view of the spatial disposition as adopted by compound (**G**), showing high binding affinity and considered to characterize the ‘active conformation(s)’ by which the molecule might interact with the cyclodextrin structure. High level quantum chemical approaches were also used to better define the conformation of the carbohydrazide moiety (Scheme 1) checking the soundness of the molecular mechanics performance.^{22–24}

A further aspect of the study was motivated by the analysis of the acceptor character of the sulfonamide^{25–31} group then extending to the *non standard* CH–O hydrogen bonds. The latter type of hydrogen bonds and directional C–H... π interactions were detected in a number of CD inclusion complexes, as also supported by structural evidences.¹⁷ The typical energies of C–H...O and C–H... π hydrogen bonds depend on

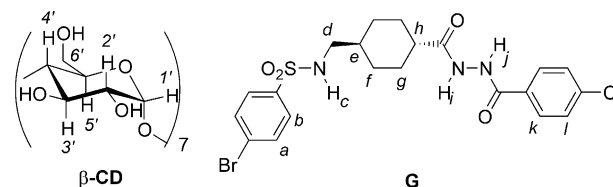


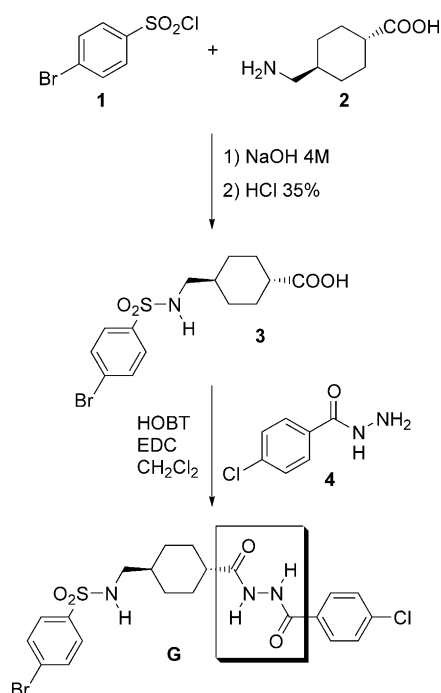
Figure 3. β -Cyclodextrin (β -CD) and guest (**G**) structure.

the nature of the C–H donor. For the very weakly polarized methyl donors, C–H...O bond energies are around 0.5 kcal/mol, not much above the energies of van der Waals interactions. For strongly polarized C–H groups like in chloroform or in terminal alkynes, C–H...O energies may be larger than 2 kcal/mol. For the other types of C–H donors, hydrogen bond energies are in between these extremes. The C–H groups forming the surface of CDs cavities, C-3–H and C-5–H, are of a significantly activated type.

Searches of the Cambridge Structural Database (CSD)^{32–34} version 5.24, November 2002. (Data updates April 2003) and the Brookhaven Protein Databank (PDB)^{35,36} were merged with Density Functional Theory (DFT)^{37–42} results (data not shown).

2. Results and discussion

Trans-*N*-{4-[*N'*-(4-chlorobenzoyl)hydrazinocarbonyl]cyclohexylmethyl}-4-bromobenzenesulfonamide (**G**) was prepared (Scheme 1) by reaction of *trans*-4-[(4-bromobenzenesulfonyl)aminomethyl]cyclohexanecarboxylic acid (**3**) with 4-chlorobenzoic hydrazide (**4**). The intermediate **3** was prepared from 4-bromobenzenesulfonyl chloride (**1**) and *trans*-4-(aminomethyl)cyclohexanecarboxylic acid (**2**). The formation of the sulfonamide **3** was carried out according to the Schotten–Baumann method in 4M NaOH. Afterwards, the desired carboxylic acid is obtained by a dropwise adding of 35% HCl. The formation of the corresponding carbohydrazide **G** was carried out by activating the corresponding carboxylic acid with 1-ethyl-3-(3'-dimethylaminopropyl)carbodiimide (EDC). In order to avoid the formation of *N*-acylurea, the reaction is car-



Scheme 1. Synthetic route to **G**. The computationally investigated uncommon bound is squared.

ried out at 0°C, in the presence of 1-hydroxybenzotriazole (HOBT) to entrap the intermediate (*O*-acylisourea) so hampering the intramolecular re-ordering which could lead to the *N*-acylurea.

The ¹H NMR spectrum (Fig. 4) of **G-Na** (5 mM, D₂O) was assigned by comparing the interproton scalar and dipolar correlations drawn from the COSY and ROESY maps, respectively.

The characterization data are reported in Table 1.

As a starting point for the assignment of the disubstituted cyclohexane ring, we used the methylene protons *d* of the substituent in 1-position, the resonances of which are well recognizable at 2.40 ppm. These are *J* coupled to the proton originating the signal at 1.11 ppm, which must be *e*, the scalar correlations of which lead to the pairs of vicinal protons named as *f*, at 0.66 and 1.60 ppm. The other proton at 2.03 ppm, integrating for 1H, must be assigned to *h*, which is *J* coupled to the two pairs of vicinal protons at 1.20 ppm and 1.65 ppm, indicated as *g*. Among the *f* and *g* couples, those at 0.66 and 1.20 ppm were attributed to the axial ones (Fig. 5) as each of them generates dipolar interaction (Fig. 6) on only one pair of protons *g* and *f* respectively adjacent to them. Therefore, the other two couples at 1.60 and 1.65 ppm are *f*-equatorial (*f*_{eq}) and *g*-equatorial (*g*_{eq}) respectively.

The relative stereochemistry of the two *trans*-1,4-substituents on the saturate ring was unequivocally defined on the basis of the following NOE interactions (Fig. 6): the methylene protons *d* originate NOE effects on both proton pairs *f*, axial and equatorial, whereas the proton *e* on the same site gives dipolar interactions only with the protons *f*_{eq} and *g*-axial (*g*_{ax}), therefore the substituent, which the *d* methylene protons belong to, and the *e* proton are respectively equatorial and axial as shown in Figure 5. Therefore, the other substituent must be equatorial itself; as a matter of fact the proton *h* generates dipolar interaction with *g*_{eq} and *f*-axial (*f*_{ax}), but no NOE is observed at the frequency of *g*_{ax} (Fig. 6), leading to the conclusion that *h* must be axial and, hence, the substituent on the same carbon atom is equatorial (Fig. 5).

A diequatorially (Fig. 7) substituted lowest energy conformer was also found by HF-MIDI (Hartree–Fock)^{23,24} calculations. The amide shows a good delocalization of each N lone pair into an anti C–N σ*. There are some soft torsions for the phenyl rings to rotate, but the phenyl conformation is pointless and it

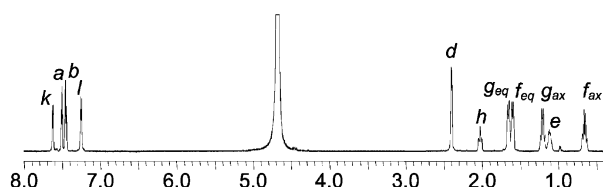


Figure 4. ¹H NMR spectrum (600 MHz, D₂O, 5 mM, 25 °C) of **G-Na** (scheme numbering in Fig. 3).

can adopt whatever position is required by the host. The delocalization is indeed into a σ^* orbital by a kind of anomeric effect or to be a bit careful ‘generalized anomeric effect’ since this isn’t oxygen lone pair delocalization into a C–O σ^* .⁴³ Each nitrogen is π delocalized within its own amide, but it is σ delocalized to the other. Basing on the antiperiplanar relationship between the nitrogen lone pairs in the pyramidal nitrogens and the corresponding C–N bonds [–C(1)–N(2)–N(3)–C(4)– where C(1) and C(4) are the carbonyl carbons], the anomeric delocalization is $n[\text{N}(3)] \rightarrow \sigma^*[\text{C}(1)–\text{N}(2)]$ and $n[\text{N}(2)] \rightarrow \sigma^*[\text{C}(4)–\text{N}(3)]$. Such anomeric delocalization of the nitrogen lone pairs is often invoked in phosphoramides and heterocycles including endocyclic amide nitrogens.^{43,44}

Within the aromatic protons, which produces four well resolved resonances between 7.00 and 8.00 ppm, those belonging to the *p*-bromophenyl group were easily assigned as the methylene protons *d* originate a weak but observable NOE at 7.45 ppm (Fig. 6), which can be attributed to the proton pair *b* adjacent to the sulfonamide function. These last are *J* coupled to the protons *a*, at 7.51 ppm, which are in *ortho* position to the bromine. The assignment of the aromatic protons of the other

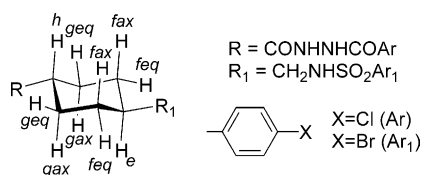


Figure 5. Cyclohexane conformational arrangement.

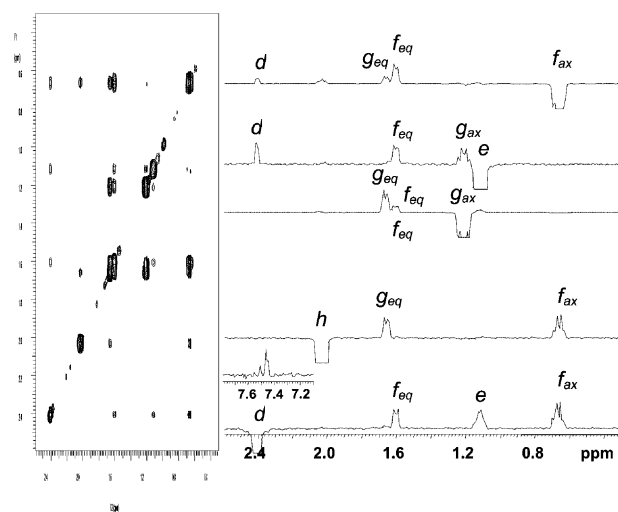


Figure 6. 2D ROESY map (600 MHz, D₂O, 5 mM, mix 0.4 s, 25 °C) of **G-Na**: aliphatic region.

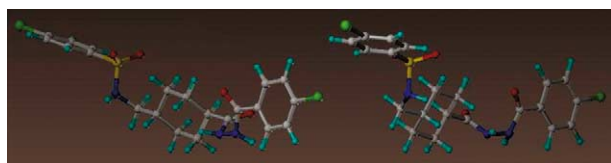


Figure 7. Most stable (orthographic view) diequatorially substituted conformer as calculated by the MIDI Hartree–Fock (HF). See text for explanation.

aromatic ring was achieved by analysing the 2D ROESY map of **G** in its acidic form in DMSO-*d*₆, where the exchangeable amide protons, which are not detectable in D₂O, produce three well-resolved resonances at 7.71, 9.81 and 10.35 ppm (Table 1). Of these, the resonance at 7.71 ppm has been assigned to the sulfonamide NH proton on the basis of its inter-NOE with the methylene protons *d*. The two high frequency shifted protons give dipolar interaction with the highest frequency aromatic proton at 7.86 ppm, which has been assigned to the aromatic protons named as *k* (Table 1). Analogously, the highest frequency aromatic protons at 7.62 ppm in D₂O have been assigned to the protons *k* and, finally, the protons *l* are those producing the signal at 7.25 ppm in D₂O. Since no dipolar interactions are observed between the aromatic protons and the aliphatic protons of the cyclohexane ring, the compound **G** must assume in solution an ‘extended’ conformation like that shown in Figure 8a.

In the presence of β -cyclodextrin an about three fold increase of the solubility of **G-Na** is achieved allowing us to analyse a 12 mM equimolar mixture **β -CD/G-Na** and in the corresponding ¹H NMR spectrum chemical shift variations (Table 1) are measured, which are markedly superior for the methylene protons *d* and for the cyclohexane ring nuclei, *f*_{eq} and *g*_{eq} in particular. In order to ascertain whether these variations are simply due to complexation effects or to conformational transitions as a result of complex formation, we analysed the 2D ROESY maps of the mixture at mixing times variable from 0.1 s to 0.8 s. The intramolecular NOEs detected in the mixture are similar but not equal with respect to those found for the free **G-Na**, as the aromatic protons *b* of the *p*-bromophenyl moiety show dipolar interactions with the cyclohexane ring protons *e* and *f*. Since the same aromatic protons do not originate any NOE on the protons *g*, we must hypothesize that a folding of the chain occur as a consequence of the

Table 1. ¹H NMR chemical shift data (δ , ppm referenced to TMS as external standard) of **G** in DMSO-*d*₆ and **G-Na** in D₂O in the pure form (5 mM) and in the equimolar mixture (12 mM, D₂O) with β -cyclodextrin (**β -CD**). Complexation shifts ($\Delta\delta = \delta_{\text{mixture}} - \delta_{\text{free}}$, ppm) for the **G-Na** protons in the presence of equimolar amount of **β -CD**

Proton	G ^a		G-Na ^b		G-Na/ β -CD ^b		$\Delta\delta \times 10^2$
	δ (ppm)	m	δ (ppm)	m	δ (ppm)	m	
<i>a</i>	7.81	d	7.51	d	7.52	d	6
<i>b</i>	7.71	d	7.45	d	7.44	d	–6
<i>c</i>	7.71	s					
<i>d</i>	2.59	br. s	2.40	d	2.31	m	–54
<i>e</i>	1.30	br. s	1.11	br. s	1.14	br. s	18
<i>f</i> _{eq}	1.73	br. d	1.60	br. d	1.67	m	42
<i>f</i> _{ax}	0.86	br. q	0.66	br. q	0.64	m	–12
<i>g</i> _{eq}	1.76	br. d	1.65	br. d	1.75	br. d	60
<i>g</i> _{ax}	1.31	br. q	1.20	br. q	1.25	br. q	30
<i>h</i>	2.15	br. t	2.03	br. t	2.03	br. t	0
<i>i</i>	10.35	br. s					
<i>j</i>	9.81	br. s					
<i>k</i>	7.86	d	7.62	d	7.64	d	12
<i>l</i>	7.56	d	7.25	d	7.25	d	0

^a 300 MHz.

^b 600 MHz.

interaction with the cyclodextrin, bringing the *p*-bromophenyl ring approximately perpendicular to the cyclohexane plane. Furthermore, the inter-NOE $e-g_{ax}$ is more intense than it is for the pure compound (compared to the other intramolecular effects produced by the proton *e*) to indicate a ring distortion consequent the chain folding (see Fig. 8b for a picture of **G-Na** in the complexed state). Dipolar interactions (Fig. 9) are observed among all **G-Na** protons and the internal protons $H_{3'}$ and $H_{5'}$ of the cyclodextrin, respectively located on its wider and narrower internal surface, according to the formation of inclusion complexes. In our case the relative intensities of the inter-NOEs produced on $H_{3'}$ and $H_{5'}$, which well reflect the orientation of **G-Na** into the macrocycle, cannot be explained by means of one kind of inclusion complex only, but different complexes or complexes having stoichiometry different from the one to one must be present.

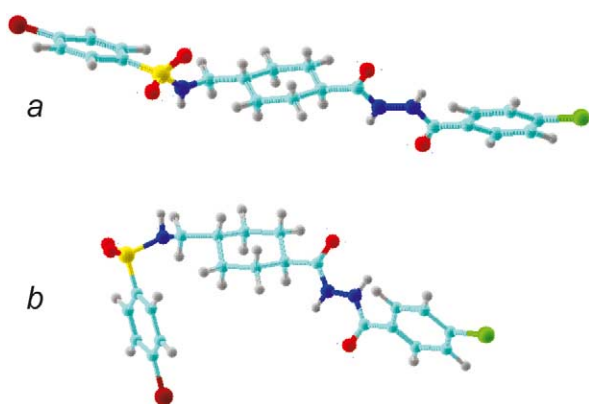


Figure 8. Conformational arrangement of **G-Na** in D_2O solution in the pure (a) and complexed (b) form.

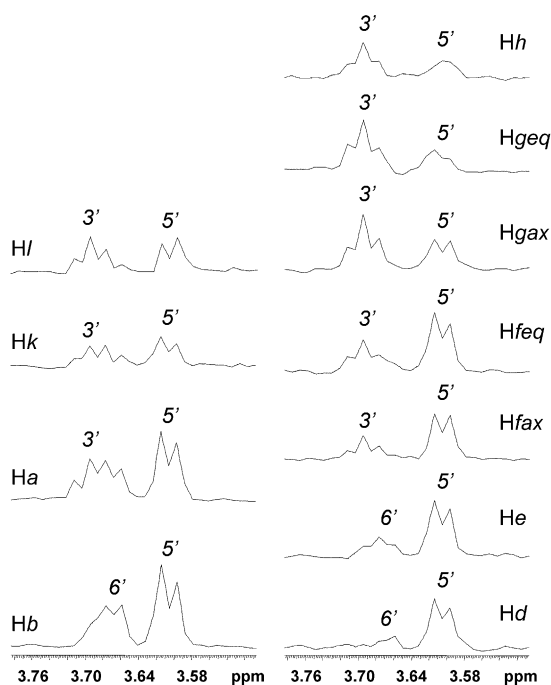


Figure 9. 2D ROESY (600 MHz, D_2O , 12 mM, mix 0.4 s, 25 °C) analysis of **G-Na**/β-CD (1:1). Spectral region including the cyclodextrin protons of the traces corresponding to **G** protons.

Although some slight differences in the shape can arise from the two combined approaches the folded more stable complexed conformer (Fig. 8b) as found by NMR is conceptually in good agreement with the computational result 'in vacuo' mimicking the apolar CD's cavity. Contrary to the solution NMR (Fig. 8a) where no possibility of overlapping by π -clouds interactions of the two aromatic seems to be, a substantially folded, a slightly solvation energy *stretched* structure, was also found in the *aqueous* conformational (Fig. 10b) analysis by the software MACROMODEL (version 8.0).²² Provided that *false* minima might come out from the calculation itself, the two computationally detected folded conformations (Fig. 10a and b), the substantial difference of which lies in the spatial location of the freely rotating *p*-chlorophenyl group, may represent two active forms fitting the hydrophobic cavity of the carbohydrate 'receptor', that is, allowing maximum contact between the hydrophobic part of the guest molecule and the internal surface of the CD cavity, and finally leading to one of the two complexes detected by the NMR investigation (see below).^{8,17} Interestingly a higher energy (−34.92 KJ/mol vs −36.74 KJ/mol) conformer *aligning* very well with that linear detected by NMR was also found by the software MACROMODEL (version 8.0).^{21,22} The partial fitting of the linear form (Figs 8a and 10c) in the cyclodextrin cavity further supports the above computational result and the proposed dynamic view of the interaction by a reverse *switch on* mechanism (from an inactive unfolded to an active folded) leading to the folded conformer as that active.^{45,46} Both the folded conformations might be stabilized by π clouds interactions between the two aromatic rings.

According to the folded structure having the *p*-bromophenyl group faced to the saturate ring, the methylene protons *d*, the ring proton *e* and the aromatic protons *b*, which are in close proximity each other in the folded

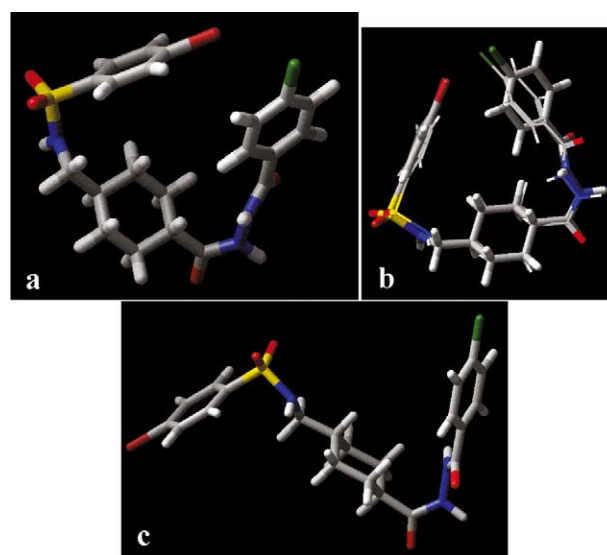


Figure 10. (a) In vacuo lowest energy conformer of compound **G** as obtained by Macromodel 8.0;^{21,22} (b) superposition of the in vacuo (wire) and the aqueous (capped sticks) lowest energy conformers; (c) higher energy (−34.92 KJ/mol) aqueous conformer as obtained by Macromodel 8.0.^{21,22} See the text for further details.

structure (Fig. 8b), produce NOEs only on the protons $H_{5'}$ and $H_{6'}$ (Fig. 9) respectively located on the narrower internal and external surface, whereas the protons a , which are on the same aromatic moiety, and the protons f_{ax} and f_{eq} also determine a dipolar interaction with the internal protons $H_{3'}$ at the wider part of the truncated cone (Fig. 9). Accordingly, for the cyclohexane protons g_{ax} or g_{eq} and the proton h the NOE effect at the $H_{3'}$ frequency is more intense with respect to that one observed at the $H_{5'}$ frequency (Fig. 9). Therefore, the **G-Na** substrate, in its folded structure, is included into the cyclodextrin as shown in Figure 11a, once again in agreement with the conformational analysis which shows a folded conformation (Fig. 10a and b) underlying a backwards mechanism to that commonly assumed for the active forms of proteins⁴⁵ and GPCR (G-Protein Coupled Receptor Ligands) ligands,⁴⁶ that is, a reverse *switching on* mechanism.⁴⁶

It might be further speculated on the CDs as receptor mimic to profile the possible ligand changes or the mutual ligand–receptor induced fit before binding.^{45–47}

On the other hand, the aromatic protons k and l of the *p*-chlorophenyl moiety produce comparable NOEs on the protons $H_{3'}$ and $H_{5'}$ (Fig. 9) and hence are themselves completely included into another unit of cyclodextrin in the same complex or in a different complexed form. Taking into account that the proton h , which can be included into both cyclodextrin units, shows a largely prevalent interNOE with the protons $H_{3'}$ (Fig. 9), the part of the molecule bearing the *p*-chlorophenyl ring is included into the cyclodextrin from its larger rim (see Fig. 11b).

The presence of a 1 to 2 complex **G-Na/β-CD** can be ruled out on the basis of the determination of the complexation stoichiometry and of the proton selective relaxation measurements.

By using the continuous variation method (Job's method)¹⁸ applied to different protons of **G-Na** in mixtures with the cyclodextrin having the same total concentration but different molar ratios, the corresponding Job plots are nearly symmetrical curves with a max-

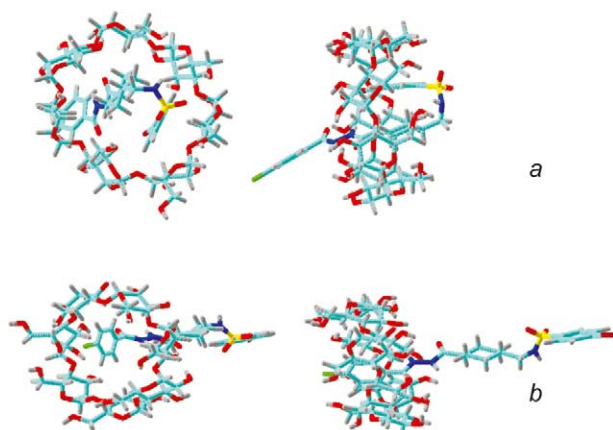


Figure 11. Conformational arrangement of the two 1:1 **G-Na/β-CD** inclusion complexes as derived by NOE analysis.

imum at the molar fraction of 0.5 corresponding to a 1:1 stoichiometry (Fig. 12). Therefore, there is simultaneous presence of two different 1:1 complexed forms of **G-Na**. The slight asymmetries of the curves are probably due to the fact that the chemical shifts variations are originated by the formation of the two different complexes of Figure 11, each having 1:1 stoichiometry, but with different stabilities.

As the formation of 1:1 against 1:2 **G-Na/β-CD** complexes should affect the dynamic features of the cyclodextrin severely, we determined the interproton cross-relaxation rates σ_{ij} of **β-CD** to compare its reorientational correlation times in the presence of **G-Na** or in the free state. In the initial rate approximation,⁴⁸ this parameter, which describes the magnetization transfer between the spins i and j , depends on the internuclear distance r_{ij} and on the reorientational correlation time τ_c of the vector ij :

$$\sigma_{ij} = 0.1\gamma^4\hbar^2r_{ij}^{-6}\tau_c\left[\frac{6}{1+4\omega^2\tau_c^2}-1\right] \quad (1)$$

where γ is the gyromagnetic ratio, ω is the proton Larmor frequency, and \hbar is the reduced Planck's constant.

For a proton pair having a near fixed distance r_{ij} , in a molecule moving in the extreme narrowing limits ($\omega^2\tau_c^2 \ll 1$), the cross-relaxation rate becomes a simple increasing function of the reorientational correlation time:

$$\sigma_{ij} = 0.5\gamma^4\hbar^2r_{ij}^{-6}\tau_c \quad (2)$$

Whereas, when the motion slows down to the $\omega^2\tau_c^2 \gg 1$ region, σ_{ij} shows still a linear dependence on τ_c but it is negative:

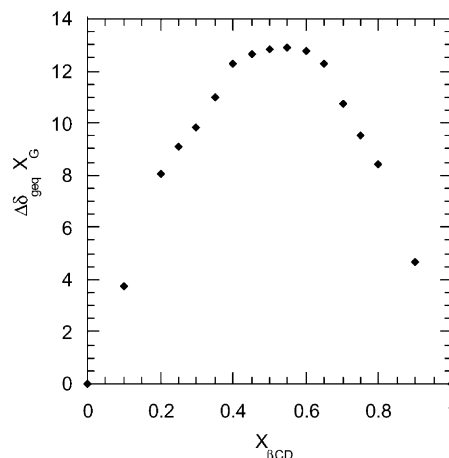


Figure 12. Job plot for **G-Na/β-CD** mixture. Protons g_{eq} of **G-Na** was used as the diagnostic protons, and the total concentration was 5 mM.

$$\sigma_{ij} = -0.1\gamma^4\hbar^2 r_{ij}^{-6} \tau_c \quad (3)$$

Hence, σ_{ij} can be employed as a probe of the dynamic changes, which occur in a molecule as a consequence of the aggregation to another molecule. Among the available experimental methods to determine σ_{ij} , we selected the one based on the determination of proton mono- (R_i) and biselective (R_{ij}^i) relaxation rates:

$$\sigma_{ij} = R_{ij}^i - R^i \quad (4)$$

Monoselective relaxation rates are measured by following the recovery of the signal of the spin i selectively inverted, by leaving unperturbed all the other spins in the molecule; the biselective relaxation rates are determined under conditions of simultaneous inversion of the proton pair ij . Therefore, we measured the monoselective relaxation rate of the proton $H_{2'}$ of the cyclodextrin as 1.04 s^{-1} in the pure compound, slightly increasing to 1.23 s^{-1} in the mixture with **G-Na** (Table 2). The biselective relaxation rate of the same proton under simultaneous inversion of the proton $H_{1'}$ ($R_{2'1'}^2$) underwent a similar slight increase from 0.89 s^{-1} (pure cyclodextrin) to 1.07 s^{-1} (mixture). From these values we calculated the cross-relaxation rates for the proton pair $2'1'$ of -0.15 s^{-1} and -0.16 s^{-1} in the pure and complexed cyclodextrin, respectively. On the hypothesis that the intramolecular distance $r_{2'1'}$ is not affected by the complexation significantly, the ratio between the two above cross-relaxation terms should reflect the ratio between the reorientational correlation times of the proton pair $2'1'$ in the mixture and in the pure compound. In our case this ratio is very close to 1 and hence only 1 to 1 complexes can be present in solution. As a matter of fact, as previously demonstrated,⁴⁹ on formation of an inclusion complex containing two units of cyclodextrin, the molecular motion of the macrocycle should slow down remarkably.

Therefore, we can conclude that the complexation process of **G-Na** by the cyclodextrin, responsible for the observed solubility increase, involves the formation of two different 1 to 1 inclusion complexes, both having the drug included from the wide rim of the macrocycle (Fig. 11). In one complex, the *p*-chlorophenyl group penetrates into the cyclodextrin, probably due to the attractive driving 'hydrophobic'^{12,13} interaction between the apolar cavity (Figs 1b and 2a and b) and the aromatic moiety assisted by the formation of hydrogen bonds among the NH–CO groups of the substrate and the secondary hydroxyls of the cyclodextrin (Fig. 11b). Generally speaking, polar atoms on the surface of a molecule contribute to its selectivity, and hydrophobic atoms give it its affinity.

Table 2. Mono- (R^2 , s^{-1}), biselective ($R_{2'1'}^2$, s^{-1}), cross-relaxation ($\sigma_{2'1'}$, s^{-1}) rates and reorientational time (τ_c , s) for the $2'1'$ protons of β -cyclodextrin in D_2O in the pure and complexed state

	R^2	$R_{2'1'}^2$	$\sigma_{2'1'}$	$\tau_c (10^{-10})$
β -CD	1.04	0.89	−0.15	4.85
G/ β -CD	1.23	1.07	−0.16	5.17

The nitrogen lone pairs which may be delocalized into the amide carbonyl and do not have to be planar to conjugate are also somewhat delocalized into adjacent C–N antibonding σ^* orbitals being available to serve as weak H-bond acceptors in an active site. Those nitrogen atoms would be expected to be rather flexible about their chemical behavior.

The formation of the other complex brings about a change of the conformation of **G-Na** from the linear structure of Figure 8a to the folded one having the *p*-bromophenyl plane bent at the cyclohexane ring and perpendicular to it (Fig. 8b).^{45,46} Probably this kind of folding allows the simultaneous deep penetration of the apolar saturated and aromatic rings into the cyclodextrin, indicating the relevance of the van der Waals and hydrophobic interactions that are mainly dependent on such structural features. These interactions are the main cause for the deep penetration of benzene derivatives into the cavity of the CD that is mainly apolar and hydrophobic. The sulfonamide group protruding from the narrower part of the cavity, works as an *auxiliary* hydrogen bonds acceptor to stabilize the complex by attractive interactions with the primary hydroxyls (Fig. 11a).^{17,25–31}

In bioorganic chemistry, the effectiveness of sulfonyl and sulfonamide oxygens as good hydrogen-bond acceptors likewise carbonyl or hydroxyl oxygens is frequently questioned. The relevant properties can be directly determined or inferred from experimental structural data.^{32–34} Further structural comparisons, and direct energetic comparisons, are possible with high level quantum chemical approaches.^{25–31,37–42} Results from an extensive Cambridge Structural Databases (CSD)^{32–34} (Fig. 13) and Brookhaven Protein Databank (PDB) entries^{35,36,49,50} support the role of the sulfone group as an acceptor in biological complexes. From a total of 2316 hits (1261 inter- and 1135 intramolecular) as found in the CSD database,^{32–34} 1346 (58%) are represented from unique (not duplicates) hits with a percentage of 39.96 and 60.04 for intra- and intermolecular

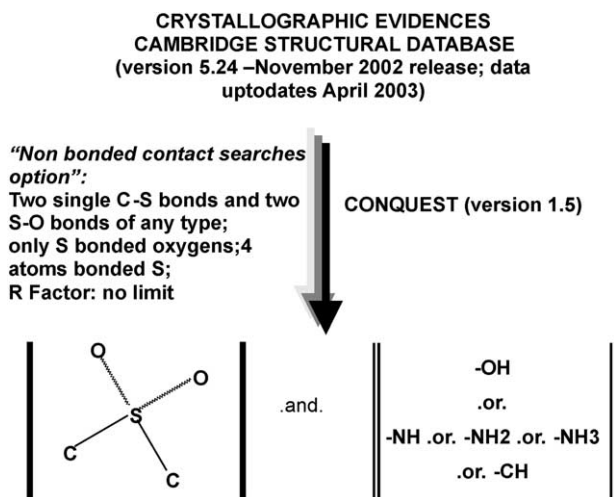


Figure 13. Search criteria in the Cambridge Structural Database using the 'Non Bonded Contact Searches' option (version 5.24, November 2002 release; data uptodates April 2003).

hydrogen bonds, respectively. A percentage of approximately 20% hydrogen bonds of all hits was guessed as directional.

Density Functional Theory (DFT) calculations using the B3LYP methodology^{37–42} provide useful comparisons with the carboxyl group to further support this role (data not shown). On the other hand this complex can be also stabilized by the hydrogen bond interactions between the NH–CO groups protruding from the wide rim of the cyclodextrin and the secondary hydroxyls of the macrocycle as above discussed. Hydrogen bonds can also be formed with the primary O-6 hydroxyl groups which are placed at the narrower of the two cavity openings. The interglycosidic O-4 atoms are sterically poorly accessible, and serve only occasionally as acceptors of O–H...O hydrogen bonds. O/N–H...O hydrogen bonds with either hydroxyl groups or O-4 atoms are often regarded as the only possible host-guest hydrogen bonds in CD inclusion complexes. If polar guest molecules are included in the CDs cavities, they have limited opportunity to satisfy their hydrogen bond potentials. Typically, guest molecules carrying hydroxyl groups are oriented in such a way that hydrogen bonds can be formed through the cavity openings to neighbouring CD or crystal water molecules.¹⁷

A survey of the Brookhaven Protein Databank (PDB) for donor, C–H...X interactions revealed more than 500 high-resolution structures with a 30% of kinase aromatic ligands complexes.^{36,50,51} Arrangements involving weak hydrogen bonds are more prone to disorder than those stabilized by conventional hydrogen bonds: the entropy gain due to disorder can easily exceed the enthalpy loss due to breaking the weak hydrogen bonds.¹⁷

Overall the depicted dynamic process of binding between the β -cyclodextrin and the guest molecule results from a subtle interplay between steric conditions, the hydration of the free species and the complexes, van der Waals interactions, dipole–dipole interactions, hydrogen bonding, and mutual conformational changes of the interacting molecules. The complexation of the β -cyclodextrins with *benzene* type derivatives, which penetrate deeply into the apolar and hydrophobic cavity of the host, is controlled by topological and topographic parameters indicating the relevance of the van der Waals and hydrophobic interactions.¹⁷

3. Experimental

3.1. General methods

All the new compounds were characterized by elemental analysis and ¹H NMR. The ¹H NMR spectrum of **3** was obtained on a Bruker Model AC-200E (200 MHz) with Me₄Si as the internal standard. Thin layer chromatography was performed on aluminum sheets precoated with silica gel (HF 254, Merck). The developed chromatograms were viewed under UV light or iodine revelation. Melting points were determined on a Mettler

FP82 hot stage apparatus equipped with a FP800/FP80 processor and an Olympus 8091 microscope provided with a video system and were uncorrected. Microanalysis of *vacuum*-dried samples were obtained on a Carlo Erba 1106 elemental analyzer (over P₂O₅ at 1–2 mmHg, 24 h at 60–80 °C). Results are within 0.4% of theoretical values unless otherwise indicated.

The ¹H and ¹³C chemical shift data directly concerned with the subject study of **G** in DMSO-*d*₆ were further obtained using a Varian VXR300 spectrometer operating at 300 MHz and 75 MHz for ¹H and ¹³C, respectively. ¹H and ¹³C NMR chemical shifts are referenced to TMS as external standard. All NMR spectra in D₂O were recorded on a Varian INOVA600 spectrometer operating at 600 MHz for ¹H using a 5-mm broadband inverse probe with *z*-axis gradient. The sample temperature was maintained at 25 °C. The 2D NMR spectra were obtained by using standard sequences. Proton gCOSY 2D spectra were recorded in the absolute mode acquiring eight scans with a 3-s relaxation delay between acquisitions for each of 512 FIDs. The ROESY (Rotating-frame Overhauser Enhancement Spectroscopy) spectra were recorded in the phase-sensitive mode, by employing a mixing time ranging from 0.1 to 0.8 s. The spectral width used was the minimum required in both dimensions. The pulse delay was maintained at 8 s; 512 hypercomplex increments of eight scans and 2K data points each were collected. The data matrix was zero-filled to 2K×1K and a Gaussian function was applied for processing in both dimensions. The selective relaxation rates were measured in the initial rate approximation⁴⁸ by employing a selective π pulse at the selected frequency. After the delay τ , a non-selective $\pi/2$ pulse was employed to detect the longitudinal magnetization. For the bisselective measurements, the two protons were inverted consecutively. Each selective relaxation rate experiment was repeated at least four times.

All the conformational and modelling studies were carried out on a SGI-R5000 and-OCTANE workstations operating under IRIX 6.5.+ using the software Macro-model (version 8.0)^{21,22} as implemented in the version 5.0 of the MAESTRO suite.^{21,22} The **G** structure was built by the Macromodel fragment library. Default parameters were used except of a lower convergence criteria (0.001). Density Functional Theory calculations (data not shown)^{37,42} and CSD (Cambridge Structural Database) searches by the software CONQUEST (version 1.5)^{32–34} were run on a PC working under WINDOWS XP. The same *double boot* machine was also used to run the GRID21 software^{9–11} under the LINUX operating system.

The cyclodextrin structure was retrieved from the Cambridge Structural Database (CSD)^{32–34} (version 5.24, November 2002. Data updates April 2003. Codes: BCDEXD03 or BISTAY and GETPAW for the GRID21^{9–11} and HINT mappings, respectively^{12–14}). All the structures were at a resolution lower than 3.2 Å. The CSD file was exported to .pdb and read in SYBYL 6.8 or 6.9 to carefully check the coordinates and extract the co-crystallized ligand as well as to delete the water

molecules before the GRID 21 (UNIX or LINUX version)^{9–11} (Fig. 1) and HINT 2.35S (Sybyl 6.9 version)^{12–14} (Fig. 2) analyses. The atom potential types bond orders were carefully checked to evaluate their correctness with respect to the intended structure. The lack of bond order records in the PDB format necessitates that this step be diligently performed before adding possible hydrogen atoms to the ligand structure. Because hydrogen atoms are only (very) rarely located in biomacromolecular crystallographic studies, there is little experimental guidance as to their actual positions. Also worth noting is that the automated procedures to add hydrogens to biopolymers and small molecules, as in Sybyl or other software programs, often (and randomly) orient the hydrogen-bonding hydrogen atoms away from their intermolecular acceptor atoms.¹³

The default parameters of the GRID 21^{9–11} and HINT 2.35S (Sybyl 6.9 implementation)^{12–14} force fields were used.

Conformational analyses were performed using the Monte Carlo Multiple Minimum (MCMM) Search protocol as implemented in the MacroModel software.^{21,22} In the Monte Carlo approach, the *dynamic* of a molecule is simulated by randomly changing dihedral angle rotations or atom positions. Then, the trial conformation is accepted if its energy has decreased from the previous one. If the energy is higher, there are various criteria to select or not the calculated conformer. In our simulations, all of the dihedral angles of single linear bonds were allowed to move freely, and the conformation was accepted if the energy was lower than that of the previous conformation or within a fixed energy window (5 kJ/mol) as selector. Prior to submitting the ligands to the search protocol, a minimization was carried out using the MMFF (Merck Molecular Force Field) force-field as implemented in MacroModel 8.0^{21,22} with the GB/SA continuum water.^{21,22} Generally all the minimizations were performed as above reported. Default options were used with the Polak-Ribiere Conjugate Gradient (PRCG) scheme, until a gradient of 0.001 kcal Å⁻¹ was reached.

To search the conformational space, 5000 MC steps were performed on each starting conformation. Least squares superposition of all non-hydrogen atoms was used to eliminate duplicate conformations. Considering of the flexibility of the ligands under investigation, an energy cut-off of 5.0 kJ mol⁻¹, high enough to map the conformational space including the bioactive conformation, was applied to the search results. The 21 lowest energy conformers in vacuo and the eight in water within 2 kJ/mol were further optimized using the multiple minimization protocol as implemented in software MACROMODEL (version 8.0).^{21,22}

The MMFF as in the software MACROMODEL (version 8.0)^{21,22} was used for the conformational in vacuo (assumed as apolar *medium*) and *aqueous* analysis.

There are actually two MMFF implemented in MacroModel,^{21,22} namely MMFF (the default)^{52–58} and

MMFFs, where the 's' is for 'static'.⁵⁸ With the obvious exception of inversion barriers, the two force fields give similar and, when delocalized trigonal nitrogens are not involved, identical relative conformational energies. MMFF gives slightly pyramidal amide geometries and rather strongly pyramidal aniline, nucleic-acid base, and other enamine nitrogens.⁵⁸ Experimental and theoretical studies indicate that this reflects the true ground-state geometry.

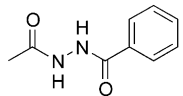
In contrast, MMFFs⁵⁸ uses modified torsion and out-of-plane bending parameters for amide or 'amide like' nitrogens, giving rise to planar or nearly planar geometries. Such nitrogens appear planar in crystal structures, due to time averaging of the rapidly inverting pyramidal geometries.

Regular MMFF is probably most useful for dynamics studies (where actual time averaging yields planar average structures), whereas the MMFFs is probably most useful for conformational search and for minimizations which are to be compared with crystallographic data.^{52–58}

The MMFF^{52–58} gives a reasonable account of the degree of pyramidalization in compound **G** and should be adequate for the intended application according to preliminary calculations (DFT B3LYP methodology with the 6-31G** basis set) by JAGUAR (version 4.0 release 23)²² on a simplified model (Table 3). Optimization of all degrees of freedom was performed in the DFT calculations, continuing until the standard gradient and energy change criteria were achieved.

Amide nitrogen geometries are notoriously hard to get right. Most are pyramidal (have some sp³ character), in spite of organic prejudice (*a bit of a myth*) to the contrary that amides are planar.⁴³ Although, there is some precedent for treating them as planar in molecular mechanics studies very few turn out to really be planar. That causes the N–H bond dipoles to oppose (*trans* conformation) one another while at the same time aligning with the other carbonyl. The pyramidal N–Hs tend to have very low barriers to inversion, so amides are a bit like proteins (it is not very meaningful to think of them as having a single 'static' structure), but instead they can adopt a range of structures all of which are quite low in energy. Thus, while the calculation says the bottom of the energy well corresponds to pyramidal nitrogen, it would probably not cost much to become planar. The hydrazine dicarbonyl, prefer to be pyramidal having a six-atom π system with eight electrons

Table 3. MMFF versus DFT-B3LYP comparison



Atom sequence	MMFF	B3LYP/6-31G**
C1–N2–N3–H5	147.5	161.6
C4–N3–N2–H6	148.8	155.5
N2–N3 distance (Å)	1.410	1.390

in it (two from each C=O plus two nitrogen lone pairs) which is to some extent like to the not so stable hexatriene dianion. Caution must be exerted in modeling G(5)-type compounds. The sulfonamide group is part of the problem, as is the C(=O)–N–N–C(=O) group. Neither of these is well parameterized in any force field. A further ‘problem’ is that the pyramidal nitrogen atoms are stereogenic being they either *R* or *S*. Unfortunately, because the inversion barrier is low, they can be either, so a large number of conformations can exist.

Actually the MMFF was designed to work best with drug-like molecules and it has good performance with the GB/SA model.^{52–58}

CONQUEST version 1.5^{32–34} was used to search the Cambridge Structural database (CSD) (version 5.24, November 2002. Data updates April 2003)^{32–34} using the ‘Non bonded contact searches’ option, criteria of which are shown in Fig. 13. Density Functional Theory calculations (DFT) were carried out using the B3LYP methodology as implemented in GAUSSIAN98^{37–42} (data not shown).

Complementary information were obtained by the softwares GRID (version 21),^{9–11} HINT 2.35S (Sybyl 6.9 implementation),^{12–14} with the additional aim to test the last code implementation of the latter software to analyze carbohydrate molecules. The capability of the HINT 2.35S^{12,13} software as implemented in SYBYL 6.9¹⁴ must be noted in correctly mapping the cyclodextrin structure in accordance with the GRID21^{9–11} software.

The GRID methodology approach^{9,11} gives a large volume of good attractive interactions, the so-called GRID-map, between the molecule and the probe. In the program Grid, a three-dimensional grid surrounds the target molecule. Version 21 of GRID works like previous versions by computing the interaction energy of a probe at every Grid point on an orthogonal matrix of points around the molecule of interest. The interaction energy between a probe and each atom of the target was then calculated for each Grid point, and this calculation generated one Grid map. By contouring the Grid map at various energy levels, one can display favorable interaction areas between the molecule and the probe as in Figure 1.

There is a GRID ‘flexibility’ option in version 21 which allows the possible rotatable chains in the test molecule to move in response to the probe. They move toward the probe when there is attraction and away from it when there is repulsion, thus simulating the response of the target to a change in its environment. This flexibility option was turned *off* in this study being no big differences in the map when the option was turned *on* as a consequence of the basket type shape structure of the cyclodextrins. GRID probes are chemical groups such as methyl, aliphatic hydroxyl, NH₃⁺ amine, water and divalent cations and the interaction energy at each Grid point is calculated between the chosen probe and every atom of the molecule. The probes are characterized by

their steric, electrostatic and hydrogen-bonding properties and by their hybridization.^{9–11}

The hydrophobic probe is attracted by dispersion and induction forces, but avoids polar atoms like hydroxyl or amine or carboxyl. An important allowance is also made for the entropic component of hydrophobicity. It must be noted that polar probes give quite large energies over quite small regions, whether the hydrophobic probe gives weaker energies over big regions of the molecular surface.^{9–11} Generally speaking, polar atoms on the surface of a molecule contribute to its selectivity, and hydrophobic atoms give it its affinity (see below).

The basis of the HINT model is that quantitatively significant data of biomolecular association are encoded in the experimental determination of hydrophobicity, particularly from the water–octanol system (LogP). The constant, LogPo/w, is a thermodynamic quantity representing the free energy of solvent transfer for partitioning between the two solvents. As such, it includes the effects of entropy, solvation, and enthalpic terms such as hydrogen bonding, Coulombic attractions, and hydrophobic attractions. It is an intuitive model because the components of the HINT score are directly related with the type of interactions present between different molecules, and the magnitude of the score is indicative of the strength of the potential interaction. Because LogP can be directly correlated with free energy, the HINT score reveals information not only about enthalpy but also about entropy. This is because a large proportion of entropy in the biological environment resulting from biomolecular associations arises from the transfer of the solute (ligand) from the solvent (water) to bound position. Concomitant with that process are the transfer proteins that bind ligands with different structures and polarity.^{12–14}

A highly exhaustive study on both the HINT paradigm, its user guidance rules and potential was recently reported by Cozzini et al.¹³

3.2. Materials

All starting materials were either commercially available or reported previously in the literature unless noted. β -cyclodextrin was purchased from Fluka.

Synthesis of *trans*-4-[(4-bromobenzenesulfonyl)aminomethyl]cyclohexanecarboxylic acid (**3**). A solution of 4-bromobenzenesulfonyl chloride **1** (6.5 g, 25.44 mmol) was added, alternately and portion wise to a solution of *trans*-4-(aminomethyl)cyclohexanecarboxylic acid **2** (4.0 g, 25.44 mmol) in NaOH 4 M (15 mL), with stirring for 30 min. After the addition, the mixture was stirred for 24 h, at room temperature. The aqueous layer was washed with CH₂Cl₂ (3×20 mL), and acidified with HCl (c) to pH 1–2. The residue obtained was filtered and washed with H₂O (5×20 mL) and *n*-hexane (5×20 mL) in order to obtain **3** as a white solid (% Yield: 21; mp, °C: 183–184). ¹H NMR (DMSO-*d*₆, 200 MHz) δ 1.15 (m, 4H), 1.75 (m, 5H), 2.05 (t, 1H, *J* = 1.4 Hz), 2.55 (s, 2H), 7.68 (m, 3H), 7.78 (d, 2H, *J* = 8.2 Hz) ppm.

C₁₄H₁₈BrNO₄S: calcd C, 44.69; H, 4.82; N, 3.72. Found: C, 44.51; H, 4.83; N, 3.58.

3.2.1. Synthesis of *trans*-N-{4-[N'-(4-chlorobenzoyl)hydrazinocarbonyl]cyclohexylmethyl} - 4 - bromobenzenesulfonamide (G). A mixture of **3** (0.8 g, 2.00 mmol) and HOBT (0.3 g, 2.9 mmol) in dry CH₂Cl₂ (25 mL) at 0 °C, under N₂, was treated with EDC (0.4 g, 2.29 mmol). After 1 h at 0 °C, 4-chlorobenzoic hydrazide **4** (0.4 g, 2.27 mmol) was added. The reaction was stirred at room temperature for 24 h. The solvent was evaporated and the residue was taken up with ethyl ether (20 mL) and water (20 mL). The obtained precipitate was filtered and washed with ethyl ether (5×20 mL) and *n*-hexane (5×20 mL) in order to obtain **G** as a white solid (yield: 68%; mp 272 °C). ¹H NMR (DMSO-*d*₆, 300 MHz) chemical shift data are reported in Table 1. ¹³C NMR (300 MHz, DMSO-*d*₆, 25 °C) δ 28.6, 29.3, 36.8, 42.1, 48.7, 126.1, 128.6, 128.7, 129.4, 131.4, 132.3, 136.7, 140.1, 164.7, 174.7. C₂₁H₂₃BrClN₃O₄S: calcd C, 47.69; H, 4.38; N, 7.95. Found: C, 47.78; H, 4.45; N, 8.05.

3.3. Binding Assays

Binding assays for both receptors NPY1 and NPY5 were done as described by Duhault et al.^{59,60} In brief, for the human Y1 receptor binding assay, using iodinated Peptide YY (NEN), incubations were performed at 30 °C for 90 min with various competitors concentrations in Buffer A (Hepes/NaOH 20 mM, pH 7.4, NaCl 10 mM, KH₂PO₄ 220 mM, CaCl₂ 1.26 mM, MgSO₄ 0.81 mM and bovine serum albumin 0.1%) with SKN-MC cell membranes (50 mg of protein/mL of assay) in a total volume of 500 mL. Non-specific binding was determined in the presence of 1 mM NPY.

The reaction was then stopped by filtration, the filters (GF/B, Whatman, precoated in 0.3% PEI) were extensively washed with buffer A, and counted in a gamma counter (Packard). For human Y5 receptor binding assay, the binding was carried out with iodinated peptide YY (NEN) as follows: COS cells transfected with the human Y5 NPY receptor were lysed and the membranes prepared by differential centrifugation. These membranes contained about 2 pmol per mg of protein of this receptor. Incubations were performed in 500 mL comprising, 20 pM final of [125I]PYY in 50 mL, 400 mL of membrane suspension (0.15 mg/mL) and competitor dilutions in 50 mL, at 30 °C for 2 h.

The reaction was stopped by filtration through GF/C filters (Whatman).

Acknowledgements

We are grateful to the Minnesota Supercomputing Institute for providing computational resources in support of this work and Prof. C. J. Cramer (Department of Chemistry and Supercomputer Institute, University of Minnesota) for the helpful discussion on MIDI. Prof. Peter J. Goodford (University of Oxford, Laboratory of Molecular Biophysics) and Prof. E. G. Kellogg

(Department of Medicinal Chemistry & Institute for Structural Biology and Drug Discovery, Virginia Commonwealth University, Richmond, Va Usa) have provided valuable discussion on the softwares GRID21 and HINT2.35S (Sybyl 6.9 version), respectively. Schrodinger, Inc.²² is gratefully acknowledged for the software Jaguar v.4.0 release 23. Thoughtful advices by Prof. A. Corsaro (Department of Chemistry, University of Catania, Italy) and the support service of the Cambridge Structural Database (CSD) were appreciated. This work was supported by the Ministero della Ricerca Scientifica e Tecnologica (MURST) and CNR, Italy.

References and notes

- Inui, A. *Trends Pharmacol. Sci.* **1999**, *20*, 43.
- Stamford, A. W.; Parker, E. M. *Annu. Rep. Med. Chem.* **1999**, *34*, 31.
- Criscione, L.; Rigollier, P.; Batzl-Hartmann, C.; Rueger, H.; Stricker-Krongrad, A.; Wyss, P.; Brunner, L.; Whitebread, S.; Yamaguchi, Y.; Gerald, C.; Heurich, R. O.; Walker, M. W.; Chiesi, M.; Schilling, W.; Hofbauer, K. G.; Levens, N. *J. Clin. Invest.* **1998**, *102*, 2136.
- Youngman, M. A.; McNally, J. J.; Lovenberg, T. W.; Reitz, A. B.; Willard, N. M.; Nepomuceno, D. H.; Wilson, S. J.; Crooke, J. J.; Rosenthal, D.; Vaidya, A. H.; Dax, S. L. *J. Med. Chem.* **2000**, *43*, 346.
- Nagaaki, S.; Toshiyuki, T.; Takunobu, S.; Yuji, H.; Aya, S.; Masaaki, H.; Miki, S.; Katsumasa, N.; Yuko, K.; Hidefumi, K.; Naoko, F.; Yasuyuki, I.; Akane, I.; Akio, K.; Takehiro, F. *J. Med. Chem.* **2003**, *46*, 666.
- Wenlock, M. C.; Austin, R. P.; Barton, P.; Davis, A. M.; Leeson, P. D. *J. Med. Chem.* **2003**, *46*, 1250.
- Ventura, C. A.; Fresta, M.; Paolino, D.; Pedotti, S.; Corsaro, A.; Puglisi, G. *J. Drug Target* **2001**, *9*, 379 (and references cited therein).
- Grigera, J. R.; Caffarena, E. R.; de Rosa, S. *Carbohydr. Res.* **1998**, *310*, 253.
- Goodford, P. J. *J. Med. Chem.* **1985**, *28*, 849.
- Goodford, P. J. *J. Chemometr.* **1996**, *10*, 107.
- Molecular Discovery Ltd.: West Way House, Elms Parade, Oxford (www.moldiscovery.com).
- Kellogg, G. E.; Abraham, D. J. *Eur. J. Med. Chem.* **2000**, *35*, 651 (www.edusoft-lc.com).
- Cozzini, P.; Fornabaio, M.; Marabotti, A.; Abraham, D. J.; Kellogg, G. E.; Mozzarelli, A. *J. Med. Chem.* **2002**, *45*, 2469.
- SYBYL Molecular Modelling Software, version 6.8 and 6.9; Tripos Inc.: 1699 S-Hanley Rd, Suite 303, St. Louis, MO 63144-2913, USA (www.tripos.com).
- Cucinotta, V.; D'Alessandro, F.; Impellizzeri, G.; Vecchio, G. *J. Chem. Soc., Chem. Commun.* **1992**, *23*, 1743.
- Cucinotta, V.; Giuffrida, A.; Grasso, G.; Maccarrone, G.; Vecchio, G. *J. Chromatogr. A* **2001**, *916*, 61.
- Castro, E. A.; Barbiric, D. J. *J. Arg. Chem. Soc.* **2002**, *90*, 1.
- Homer, J.; Perry, M. C. *J. Chem. Soc., Faraday Trans. 1* **1986**, *82*, 533.
- Neuhaus, D.; Williamson, M. *The Nuclear Overhauser Effect*; WCH: New York, 1989.
- Valensin, G.; Kushnir, T.; Navon, G. *J. Magn. Reson.* **1982**, *46*, 23.
- Mohamadi, F.; Richards, N. G. J.; Guida, W. C.; Liskamp, R.; Lipton, M.; Caulfield, C.; Chang, G.; Hendrickson, T.; Still, W. G. *J. Comput. Chem.* **1990**, *11*, 440.
- Schrodinger, Inc.: 1500 S. W. First Avenue, Suite 1180

- Portland OR 97201, USA/One Exchange Place, Suite 604, Jersey City, NJ 07302, USA (www.schrodinger.com).
23. Easton, R. E.; Giesen, D. J.; Welch, A.; Cramer, C. J.; Truhlar, D. G. *Theor. Chim. Acta* **1996**, *93*, 281.
24. Li, J.; Cramer, C. J.; Truhlar, D. G. *Theor. Chem. Acc.* **1998**, *99*, 192.
25. Hohenberg, P.; Kohn, W. *Phys. Rev. B* **1964**, *136*, 864.
26. Lee, C.; Yang, W.; Parr, R. G. *Phys. Rev. B* **1988**, *37*, 785.
27. Del Bene, J. E. *J. Phys. Chem.* **1988**, *92*, 2874.
28. Del Bene, J. E. *J. Int. Quantum Chem.: Quantum Chem. Symp.* **1992**, *26*, 527.
29. Pudzianowski, A. T. *J. Phys. Chem.* **1996**, *100*, 4781.
30. Del Bene, A. T.; Person, W. B.; Szczepaniak, K. *J. Phys. Chem.* **1995**, *99*, 10705.
31. Dewar, M. J. S.; Jie, C.; Yu, G. *Tetrahedron* **1993**, *23*, 5003.
32. Allen, F. H.; Kennard, O. *Chem. Des. Autom.* **1993**, *8*, 1 and 31.
33. Allen, F. H. *Acta Cryst.* **2002**, *B58*, 380.
34. Bruno, I. J.; Cole, J. C.; Edgington, P. R.; Kessler, M.; Macrae, C. F.; McCabe, P.; Pearson, J.; Taylor, R. *Acta Cryst.* **2002**, *B58*, 389.
35. Berman, H. M.; Westbrook, J.; Feng, Z.; Gililand, G.; Bhat, T. N.; Weissig, H.; Shindyalov, I. N.; Bourne, P. E. *Nucl. Acids Res.* **2000**, *28*, 235.
36. Lovejoy, B.; Welch, A. R.; Carr, S.; Luong, C.; Broka, C.; Hendricks, T.; Campbell, J. A.; Walker, K. A. M.; Martin, R.; Van Wart, H.; Browner, M. F. *Nature Struct. Biol.* **1999**, *6*, 217.
37. Gaussian98, PC version; Gaussian: Carnegie Office Park, Bldg. 6, Pittsburgh, PA 15106, USA (www.gaussian.com).
38. Perdew, J. P.; Yue, W. *Phys. Rev. B* **1986**, *33*, 8800.
39. Becke, A. D. *J. Chem. Phys.* **1993**, *98*, 5648.
40. Adamo, C.; Barone, V. *Chem. Phys. Lett.* **1997**, *274*, 242.
41. Perdew, J. P.; Burke, K.; Ernzerhof, M. In *Chemical Applications of Density Functional Theory*; Laird, B. B., Ross, R. B., Ziegler, T., Eds.; ACS Symposium Series, 629; American Chemical Society: Washington, DC, 1996.
42. Adamo, C.; Barone, V. *J. Chem. Phys.* **1998**, *108*, 664.
43. Cramer, C. J. *J. Mol. Struct. (Theochem)* **1996**, *370*, 135.
44. Eliel, E. L.; Wilen, S. H. *Stereochemistry of Organic Compounds*; Wiley: New York, 1994.
45. Diler, D. J.; Merz, K. M. *J. Comput-Aided Mol. Des.* **2002**, *16*, 105.
46. Modica, M.; Santagati, M.; Guccione, S.; Santagati, A.; Russo, F.; Cagnotto, A.; Goegan, M.; Mennini, T. *Eur. J. Med. Chem.* **2001**, *36*, 287.
47. Testa, B.; Kier, L. B.; Carrupt, P. A. *Med. Res. Rev.* **1997**, *17*, 303.
48. Freeman, R.; Wittekoek, S. *J. Magn. Reson.* **1969**, *1*, 238.
49. Salvadori, P.; Uccello-Barretta, G.; Balzano, F.; Bertucci, C.; Chiavacci, C. *Chirality* **1996**, *8*, 423.
50. Wang, S.; Tabernero, L.; Zhang, M.; Harms, E.; Van Etten, R. L.; Stauffacher, C. V. *Biochemistry* **2000**, *39*, 1903.
51. Su, X. D.; Tadei, N.; Stefani, M.; Ramponi, G.; Pär Nordlund, P. *Nature* **1994**, *370*, 575.
52. Halgren, T. A. *J. Comput. Chem.* **1996**, *17*, 490.
53. Halgren, T. A. *J. Comput. Chem.* **1996**, *17*, 520.
54. Halgren, T. A. *J. Comput. Chem.* **1996**, *17*, 553.
55. Halgren, T. A. *J. Comput. Chem.* **1996**, *17*, 587.
56. Halgren, T. A.; Nachbar, R. *J. Comput. Chem.* **1996**, *17*, 616.
57. Halgren, T. A. *J. Comput. Chem.* **1999**, *20*, 720.
58. Halgren, T. A. *J. Comput. Chem.* **1999**, *20*, 730 (and references cited therein).
59. Duhault, J.; Boulanger, M.; Chamorro, S.; Boutin, J. A.; Della Zuana, O.; Douillet, E.; Fauchere, J. L.; Feletou, M.; Germain, M.; Husson, B.; Renard, P.; Tisserand, F. *Can. J. Biochem. Physiol.* **2000**, *78*, 173.
60. Guéry, S.; Rival, Y.; Wermuth, C.-G.; Renard, P.; Boutin, J.-A. *Chem. Pharm. Bull.* **2002**, *50*, 636.